Progressive Collapse Analysis of Reticulated Shell structure under Severe Earthquake considering the Damage Accumulation Effect

Haitao Zhou[1]; Yigang Zhang [2];Feng Fu[3] C.Eng,M.ASCE; Jinzhi Wu[4]

Abstract:

A reticulated shell is one of the conventional long span space structures, prone to progressive collapse under a severe earthquake due to its unique single layer feature.

This is. However, the collapse mechanism of this type of structure is not well studied. In this paper, a numerical modelling technique using the fiber beam elements is developed. The correspondent material model based on the inclusion of damage accumulation was also developed in order to determine the failure criteria of structural members. An effective way to simulate the buckling behavior of the structural members is also used in the numerical simulation. The relevant numerical method is developed and validated against experimental tests: good agreement is achieved. Based on this numerical method, a parametric study of the reticulated shell under severe earthquake loading is performed and the responses of the structure is investigatedand a three-stages collapse mechanism of this type of structure was observed.

Key words: single-layer reticulated shell; progressive collapse; severe earthquake, cumulative damage; hysteresis curve; stiffness degradation

---

[1] *Engineer, Spatial Structure Research Center, Beijing University of Technology, Beijing,100124, China, 2Henan University of Urban Construction, Henan,467001,China. Email :Chinaazhouhaitao111111@163.com*

[2] *Professor, Spatial Structure Research Center, Beijing University of Technology, Beijing,100124, China and Key Lab of Urban Security and disaster Engineering, MOE, Beijing University of Technology, Beijing,100124, China. Email: bzyg@bjut.edu.cn*

[3] *Lecturer, School of Mathematics, Computer Science & Engineering, Department of Civil Engineering, Northampton Square, London, C1V 0HB,U.K.*

Chanbai Mountain distinguished Visiting Professor, Jilin Jianzhu University,Chanchun, JiLin, China. Email: feng.fu.1@city.ac.uk

[4] *Professor, Spatial Structure Research Center, Beijing University of Technology, Beijing,100124,China and Key Lab of Urban Security and disaster Engineering, MOE, Beijing University of Technology, Beijing,100124,China. Email: kongjian@bjut.edu.cn*

Introduction

The event of the 9/11 in 2001 embarked the research on the causes of progressive collapse in structures and possible mitigating methods. Increasing attention has been paid on the studies of collapse mechanism and collapse prevention methods of buildings in recent years. However, few studies have been performed toward the collapse mechanism and relevant collapse prevention measures for space structures. For a single layer space structures, such as the reticulated shell, stability is pressing important, as this type of structure is prone to local buckling which may initiate the dynamic global buckling and collapse of the entire structure under the severe earthquake. Therefore, the research is this area is imperative.

There are some design procedures in Europe and U.S. available on mitigating the progressive collapse of buildings, such as design guidance of the Department of Defense (DoD) (2005) and the General Services Administration (GSA) (2003) ASCE 7 (2010) in U.S; the design code of British Building Regulations (2004), BS5950 (2001) in U.K. Some references such as FEMA 2002 (2002) and NIST 2005 (2005) also provide general design recommendations, which require steel-framed structural systems to have enough redundancy and resilience. However, most of these design codes are focused on buildings; no detailed design procedure in preventing progressive collapse of reticulated shell is available.

So far, some numerical investigation (McGuiew,1974),(Powell,2004) and experimental tests Shimada et al. (2008),, Tsitos (2008) have been done on the building structures. Starossek, 2009, gave detailed introduction on the collapse mechanisms for different type of structures. Starossek, 2006, suggested a pragmatic approach for designing against progressive collapse. Brunesi et al. (2015) developed the fiber-based models for progressive collapse assessment. They integrate the incremental dynamic analysis with the Monte Carlo simulation and developed the fragility functions.

However, majority of existing research is based on the building structures, little has been noticed on the space structures. See, et al. (1986), discussed the large displacement elastic buckling of the space structures, however, they did not further investigate the collapse mechanism of the whole space structure. Deshpande (2001), discussed the collapse of the truss core sandwich beams. Orbison, et al., 1982 developed an efficient procedure for modelling the inelastic behavior of three-dimensional beam-column. Long,H.V et al. (2008), developed an efficient algorithm for both limit and shakedown analysis of 3-D steel frames by the kinematic method using linear programming technique. Ferrari et al. 2016, developed an innovative formulation of a FEM computational model for the analysis of elastoplastic 3D truss-frame structures. SHEKASTEHBAND et al., 2014 discussed the dynamic propogation of the snap-through buckling in Tensegrity structures. Blandford(1996) performed progressive analysis of inelastic space truss structures. Kato et al. (1998) discussed the collapse of semi-rigidly reticulated domes with initial geometric imperfections. Malla(2011) proposed the methodology suitable for the dynamic analysis of the progressive failure of truss structures. Fang et al. (2001) performed the simulation of the progressive collapse together with a study of suitable methods for resisting progressive collapse of single layer grid structures based on ANSYS and LS-DYNA.

In above research, damage accumulation is ignored in most of the numerical models. However, in the event of earthquake, damage accumulation can be resulted by the cyclic loading during earthquake. Therefore, when investigating the dynamic response of structure under earthquake loading, damage accumulation is essential to accurate prediction of dynamical response of structures in numerical simulation. However, little work has been done in this area.

Therefore, in this paper, based on thermodynamic theory, the damage evolution equations for fiber beam element is derived. The corresponding constitutive relationship for beam elements are also developed The relevant numerical analysis method is also developed. In addition, due to the redundancy and indeterminacy of this type of structures, dynamic instability criterion based on implicit algorithm can capture neither the collapse mechanism of the reticulated shell, nor the failure mode of individual components. Therefore, the simulation of the whole collapse process requires application of explicit dynamic algorithm which is used in this paper.

Based on above studies, a subroutine program based on explicit dynamic algorithm is developed to analyze the response of the single-layer reticulated shell under severe earthquake. The program was validated against experimental tests. It is validated that, the proposed numerical method can accurately simulate the members failure, the redistribution of internal forces and the collapse mechanism of the whole structure. Based on this numerical method, parametric studies on single layer reticulated shell is performed and the collapse mechanism of this type of structure is studied.

In this paper, the authors deal with earthquake-induced failure of some members, in most cases, global failure rather than a localized portion of structure can be observed. Therefore, the subject of this research presented in this paper is primarily to investigate the mechanism of progressive collapse rather than disproportionate collapse, which is usually considered as a special type of progressive collapse in which local failure develops causing a final disproportionate extent of damage.

Numerical algorithm development

As it is shown in Figure 1, a 3D full scale model replicating a single layer reticulated shell is set up in ABAQUS, the related numerical method is introduced in this section. The structural members used in the model are Chinese Tubular sections, with yield stress of 235MPa. The Young's modulus is 2.06×105MPa. The Poisson ratio is 0.3.

Fiber beam element method

In this research, all the structural members of the reticulated shell are simulated using the beam elements. Each beam element is further discretized into a number of longitudinal fibers across their cross-section with appropriate constitutive model defined to each fiber as it shown in Figure 2 which is the cross-section of a beam element with tubular sections. It can be seen that the beam is subdivided into 8 fibers (numbered from 1 to 8) across its cross-section. Each fiber element comprises 2 nodes with three degrees of freedom at each node. The beam element is integrated by these fibers and every section of the fiber represents one Gauss-Lobatto integration (Maerschalck et al. 2006) point. This so called fiber beam element method has been used for simulating the concrete members, (Taucer,1991) It is based on assumptions of small deformation and plane sections remain plane when load is applied. However, its application in steel members is not widely used. The overall section behavior of the beam is therefore determined by integration of the response of these 8 fibers. In another word, the constitutive relation of the cross-section of the beam element is derived by integration of the stress-strain relation of all the 8 fibers. Hence, the total response of each single beamelement under loading along the length can be further derived. The strain in each fiber is calculated based on the plane section remaining plane assumption. The stress of each fiber can be worked out from its strain value.

This fiber beam element method is used in this research to simulate all the structural members of the dome using the general-purpose program ABAQUS.

Constitutive model of the fiber and failure criterion for beam elements

In the proposed method, the cumulative damage is included. Based on strain equivalence hypothesis, the following constitutive models can be established:

In the elastic loading or unloading stage:

$$\tilde{\boldsymbol{\varepsilon}}^{e} = \tilde{\boldsymbol{\sigma}} / \boldsymbol{E} \tag{1}$$

In the plastic loading stage, the strain equivalence hypothesis is still valid, it is:

$$\boldsymbol{\varepsilon} = \tilde{\boldsymbol{\sigma}} / \boldsymbol{E}_t = \boldsymbol{\sigma} / \tilde{\boldsymbol{E}}_t \tag{2}$$

Where,

$\tilde{\varepsilon}^{e}$ Is elastic strain tensor

$\boldsymbol{\varepsilon}$ is strain tensor

σ is Cauchy stress tensor

$\tilde{\boldsymbol{\sigma}} = \boldsymbol{\sigma}/(1-\mathrm{D})$ is effective Cauchy stress tensor

$\tilde{\boldsymbol{E}} = \boldsymbol{E} \cdot (1-D)$ is effective elastic tensor;

D is cumulative damage;

$\tilde{\boldsymbol{E}}_t$ is tangent modulus.

$\tilde{\boldsymbol{E}}_t = \boldsymbol{E}_t \cdot (1 - D)$ is Effective tangent modulus;

D is the cumulative damage variable, which is an independent variable, its value increases monotonically in the plastic state. In Zhou (2010), an incremental damage evolution equation of beam element with steel material is derived according damage evolution model by Chow and Wang (1987). It is shown in Equation (3)

$$dD = \frac{1-D}{2\sigma_{11}} d\sigma_{11} \tag{3}$$

Where,

σ_{11} is axial stress existing in a fiber beam element,

Equation (3) is valid in plastic state.

Based on above theory, User Material model for the steel members was developed using the subroutine program VUMAT available from general purpose software ABAQUS, whose algorithm is as follows:

In the elastic loading or unloading stage，the stress evolution equation is:

$$\sigma_{new} = \sigma_{new}^{trial} = \sigma_{old} + \tilde{\lambda} trace(\Delta\varepsilon) I + 2\tilde{G}\Delta\varepsilon \tag{4}$$

Where σ_{new} is current stress，

σ_{new}^{trial} is trial stress，

σ_{old} is stress in the last step，

$\Delta\varepsilon$ is incremental strain，

$trace(\Delta\varepsilon)$ is Volumetric strain increment，

I is unit matrix

$\tilde{\lambda}$ and $\tilde{G}$ are two different effective lames constants:

$$\tilde{\lambda}=\frac{Ev(1-D)}{(1+v)(1-2v)},$$

$$\tilde{G}=\frac{E(1-D)}{2(1+v)} \tag{5}$$

In plastic stage, the stress evolution equation is:

$$\sigma_{new}=\sigma_{new}^{trial}-2\tilde{G}\Delta\gamma Q \tag{6}$$

Where, $\Delta\gamma$ is plastic strain increment, with

$$\Delta\gamma=\frac{1}{2G\left(1+\tilde{H}/3G\right)}\left(\left(\xi_{new}:\xi_{new}\right)^{1/2}-\sqrt{\frac{2}{3}}\sigma_0\right) \tag{7}$$

Q is Current yield surface normal tensor, with

$$Q=\sqrt{\frac{3}{2}}\frac{\xi}{\sigma_0} \tag{8}$$

And $\tilde{H}$ is effective plastic gradient,

σ_0 is yield radius,

$\xi_{new}=\sigma_{new}^{trial}-\alpha_{old}$, is difference between current trial stress and back stress with

$$\alpha_{new}=\alpha_{old}+\frac{2}{3}\tilde{H}\Delta\gamma Q \tag{9}$$

Where α_{old} is the back stress

Therefore, the damage variable D accumulatively changes as follows:

$$D_{new}=D_{old}+\frac{1-D_{old}}{2\sigma_{11}}d\sigma_{11} \tag{10}$$

Where

D_{old} is the damage value of material calculated in last sub-step and input at the beginning of current sub-step.

D_{new} is updated damage value in current sub-step.

Failure criterion of structural members

The failure criterion of each fiber is determined based on the studies by the authors in (2010). When D_{new} in a fiber develops into certain value D_{limt}, the fiber is determined as failure. Where:

$$D_{\text{limt}} = 1 - \left(\frac{f_u}{f_y}\right)^{-\frac{1}{2}}$$

In the designed VUMAT subroutine program, when the failure of one fiber is trigged, the elastic modulus of this fiber will be set as zero

automatically. When all the fibers in a beam element fail, that beam element is determined as failure, thus this beam element will be deleted by the program. After an element is deleted due to failure, the explicit dynamic equilibrium equation is used for the analysis, which is based on Central difference method of Bathe (1996) as follows:

$$M\ddot{u}_t = P_t - (I_t + I_{td}) \tag{11}$$

Where

$\ddot{u}$ is Nodal acceleration matrix,

M is diagonal matrix of mass,

P_t is matrix of external force at time t,

I_t is matrix of internal force at time t,

I_{td} is matrix of force loss due to structural elements failure

Therefore, the acceleration can be worked out as

$$\ddot{u}_t = M^{-1}\left[P_t - (I_t + I_{td})\right] \tag{12}$$

Hence, the velocity can be calculated by interpretation of the acceleration using central difference method:

$$\dot{u}_{t+\frac{\Delta t}{2}} = \dot{u}_{t-\frac{\Delta t}{2}} + \frac{\Delta t_{t+\Delta t} + \Delta t_t}{2} \ddot{u}_t \tag{13}$$

Similarly, the displacement of all the nodes at certain time can be calculated through the interpretation of the velocity.

When displacement of the fibre is determined, the strain increment of the fiber can be worked out using the displacement divided by the cross-section area of the fiber. The strain increment and initial strain will be substituted into formula (4) or (6), therefore, new stress and damage value in each fiber can be obtained by iterations.

The method of the authors (2010) is used here to simulate the buckling and post-buckling behavior. In the model, each beam element is divided into 4 segments along its length, and all the segments are arranged along a half-wave sine curve to simulate the initial imperfection.

This method is very effective in simulating the buckling and post-bulking behavior. The buckling load from the modelling result is less than 5% difference to that of the Chinese code (2003), which satisfies the requirement for earthquake analysis. Above theory is also incorporated into the subroutine VUMAT program in ABAQUS.

Validation of the numerical method

In order to validate the proposed numerical method, a full scale hysteretic test which is conducted by the first author of this paper in collaboration with Prof Li Haiwang from Taiyuan institute of technology is used here. As shown in Figure3，an arch truss with span of 5800mm，height of 1200m and depth of 300mm was tested， Chinese Tubular Section Ø88.5×3.75and Ø75.5×3.5were used for top and bottom cords，Ø60×3.25 were used for diagonal members. The grade of the steel is Chinese

Q235-B. The Arch truss was supported at the two ends with load applied at the center, as it shown in Figure 4. Tensile tests were also conducted from coupons taking from the arch truss, the material parameters are shown in Table 1. The time history of the applied load is shown in Figure 5. When applying the load, the load control method is used in the first 9 cycles, followed by displacement control in the remaining cycles.

The above tests were simulated using the numerical modelling techniques developed in this research. As it shown in Figure 6, a model replicates the full-scale test has been setup. In the simulation, the same sections for the structural members and same steel grade were selected. In addition, the same loading regime of the experimental tests was applied. The load was applied at the same position of the test, as it is shown in Figure 7, which also shows the numbering of each fiber.

The comparison of the result from the numerical modelling and full-scale test is shown in Figure 8, which shows the comparison of hysteretic curve between the test and the numerical modelling result. It can be seen that, good agreement is achieved. It can also be seen from Figure 8a that the stiffness of the structure when the vertical displacement reached16mm is smaller than that the stage that the displacement is 13mm. , This is due to the stiffness degradation resulted by Damage Accumulation. Therefore, the damage accumulation should be considered in the numerical simulation for obtaining more accurate results. The modelling result of Figure 8b also shows the similar stiffness degradation, this

proved the capacity of the proposed model to accurately capture the stiffness degradation due to the damage accumulation.

During the test, when the vertical loading displacement increase to 35mm， cracks were observed at the top chords which locate near the support as it shown in Figure 9a. With the increasing of the loading, the crack was further developing (Figure 9b), in the meantime, crack was also observed at the joints of the diagonal members, as it is shown in Figure 9 c. When the loading displacement increased to 47mm, rupture of the top chord occurred as it shown in Figure 9d. The numerical simulation also captured the similar cracking pattern.

The results of top chord member 296 and diagonal member 288 are shown in Figure 10, which are extracted from the model. As it is shown in Figure 10a, at time 334 s, when the displacement is 30 mm, the maximum value of the damage D is observed in chord member 296 and $D > D_{limt}$, which indicates the fracture of member 296. Similarly, the fracture of member 288 is also observed at time 340s when $D > D_{limt}$ is observed, as it is shown in Figure 10. the correspondent displacement was found to be 35mm in the modelling result as it is shown in Figure 11, and these two fractured members were deleted in the model by the program during the simulation.

From above comparison, it can be seen that, the proposed model can accurately simulate the response of the full-scale test.

Progressive collapse analysis under earthquake loading

In order to investigate the collapse mechanism of the reticulated dome, as it is shown in Figure 13, a 40m span single layer Kiewitt shell with 6 rings, 8 meters high, is modelled. Kiewitt shell is one of the typical grid configurations for lattice shell. As discussed in Melaragno (1991), Kiewitt shell contains the advantages of other type of shell such as Schwedler lattice shell and union type shell. Kiewitt shell has uniform grid, which contains relatively good mechanical properties such as higher bearing capacity for the seismic load. The live load of the roof is taken as 2.5KN/m^2. The dome is pin supported along the circumference. All the structural members are Chinese Steel Tubular Sections, the members in the radials are Chinese Ø 165 × 5, and the remaining sections are Chinese Ø140 × 4. The material properties are listed in Table 2.

In the simulation, all the structural members are modelled using beam elements. Each beam element is divided into 4 segments along its length to model the buckling behaviour. In addition, each beam element is sub-divided into 8 fibres across its cross-section.

The analysis is divided into two steps. The first step is static analysis, where the gravity load is applied to the structure. The second step is dynamic analysis, where the time history of Northridge earthquake (as it is shown in Figure 12) was applied at the support, in X, Y and Z direction, with the Peak Ground Acceleration (PGA) of 1600gal in X direction, 0.85 times 1600gal in Y direction and 0.65 times 1600gal in Z direction, respectively. The time duration is 15s, which is greater than 10 times the natural period of the structure.

Modelling results

Figure 13 shows the process of the collapse of the dome. It can be seen that, at 9.25s, all structural members are still in the elastic stage. At 9.75s, the GPA reaching the peak value, local structural members failure was observed at area, the local failure propagated further until 11s, when half of the dome collapsed. Figure 14 shows the sequence of the structural member failure before 11s. It can be seen that, the member failure started at the outer rings of the domes and then propagated to the center of the dome.

Figure 15 is the time history of the vertical displacement of node 1 and node 591 (their location are shown in Figure 13), where node 1 locates at the centre of apex, it can be seen that, at 12 s, the vertical displacement of node 1 increased dramatically, which indicted the collapse of the whole dome. However, node 591 experienced a two-stage collapse as it shown in Figure 15.

Figure 16 shows the response of the axial force of structural member 219 and 787 (their locations can be found in Figure 14), the two time histories are coincide at the beginning, however, element 219 drop to zero at 10.05s, element 787 is kept intact.

As it is introduced in the earlier section, the judgement of failure of the structural element is based on the value of damage accumulation of all the fibres. Figure 17 shows the stress development of the fibre number 0 and number 90 in element 219 and 787. From Figure 17a it can be seen that, the effective stress of fibre number 0 in element 219 entered yielding level after 3.37s. At 9.725s it failed, the effective stress dropped to 0. Similarly, in Figure 17b, it can be seen that, fibre number 90 failed at 10.05s. It can be concluded that, the damage accumulation is correlated to the numbers of the cyclical loading and the magnitude of the loading. From Figure 17c, it can be seen that, no failure is overserved in Element 787.

Figure 18 shows the damage value D for each fiber in element 219 and 787. It can be seen that, the value D of these fibers in element 219 all reached 0.209 before 10.05s, however, from Figure 17a and b, it can be seen that, the effective stress dropped to 0 at the final stage, which indicate the failure of the fiber. However, the maximum D value of the fibers in element 787 is only 0.104 therefore, failure is not developed.

Discussion on Collapse mechanism

Figure 13 depicts deformation and damage distribution during collapse process, where the distribution of the D value can be checked. It can be seen that, under the earthquake, the collapse process of the dome can be divided into three stages:

1. The first stage, most structural members in the dome remain as elastic, some members developed into plastic stage(0-9.5s)
2. With the accumulation of the damage developed, fracture in some structural members were observed, the stiffness of the whole structure reduced, excessive displacement was developed in local area and therefore, the subsidence of some structural members is observed in the local area.
3. The collapse is then propagated to a larger area during the time of 9.75-11s. The collapse of the whole structure started after 11s.

It can be seen that, the damage development in the structural member during these three stages are different, their deformation also varies, however, there is no sharp division can be found between these three phases.

Parametric study to investigate the collapse mechanism

In order to further study the collapse mechanism of this type of structure under earthquake loading, based on the proposed model, a parametric study is made with parameters of different span, span to depth ratio, live load, as it shown in Table 3. Two different types of shells K6 and K8 were investigated under different time history of earthquake loading and different loading input directions, as it shown in Table 3. Three time histories: Taft、El-central、Qianan（China）were chosen in the simulation. The earthquake motions were input in 0°,30°,45°,90° directions.

As it shown in Figure 19, only the modelling results of dome K8 (with span/ depth of7/1) and K6 (with span/depth 7/1) are shown here. Both have the similar collapse mechanism as it is discussed in the earlier section

The results from above parametric studies show that, very similar collapse mechanism as it shown in Figure 13 were observed. This indicates that, the collapse mechanism is not sensitive to model parameters. All the models exhibit the similar three-stages collapse pattern as it is shown in Figure 13.

Conclusion

Based on the results and analysis in this paper, the following conclusions can be drawn:

1. A new modelling technique based on fibre beam element method is developed to model the behaviour of individual structural members of reticulated shell.
2. The failure criteria of structural members based on damage accumulation theory is developed and is validated based on the full-scale tests, it shows that the proposed model can accurately simulating the stiffness degradation due to damage accumulation and failure modes of each structural member.
3. The numerical method is developed based on the VUMAT to model the global response

of a truss under cyclic loading and validated against test result, good agreement is achieved.

4. The progressive collapse analysis of single layer reticulated dome under severe earthquake is performed and the response and the collapse mechanism of single-layer reticulated shells under the severe earthquake are discovered.
5. A three-stages collapse mechanism were discovered. It is also found that this three-stages collapse mechanism is consistence for different model parameters such as: different types of the domes, different span/depth ratios, different earthquake time histories.

Reference

Bathe K J. Finite element procedures. New Jersey: Prentice-Hall, 1996

Blandford G. E., PROGRESSIVE FAILURE ANALYSIS OF INELASTIC SPACE TRUSS STRUCTURES, Computers & Structures Vol. 58, No. 5, pp. 981-990. (1996)

British Standards Institution. BS 5950: Structural use of steelwork in buildings, Part 1: Code of practice for design — rolled and welded sections, London (UK); (2001).

Brunesi E., Nascimbene R.. Parisi F, Augenti N., Progressive collapse fragility of reinforced concrete framed structures through incremental dynamic analysis, Engineering Structures, Volume 104, 1 December 2015, Pages 65-79

Chow C L, Wang J. An anisotropic theory of continuum damage mechanics for ductile fracture.Engineering .Fracture.Mechanics .Vol 27(1987), pp.33:3-16

Code for design of steel structures (GB50017),Beijing(China),2003

Deshpande V.S, Fleck N.A. Collapse of truss core sandwich beams in 3-point bending, International Journal of Solids and Structures Volume 38, Issues 36–37, September 2001, Pages 6275-6305.

Fang Y. L., Zhao Z. Z, Numerical Simulation of Progressive Collapse and Study of Resisting Progressive Collapse of Spatial Grid Structures Based on ANSYS/LS-DYNA, Advanced Materials Research, Volumes 243 – 249, (2011),pp6202-6205.

Federal Emergency Management Agency (FEMA) FEMA 403, World Trade Center Building Performance Study: Data Collection, Preliminary Observations, and Recommendations. Washington, DC, USA.,2002.

Ferrari,R, Cocchetti C, Rizzi, E (2016): Limit Analysis of a historical iron arch bridge. Formulation and computational implementation, COMPUTERS AND STRUCTURES, vol.175, pp.184-196.

GSA. Progressive collapse analysis and design guidelines for new federal office buildings and major modernization projects. The U.S. General Services Administration; (2003).

Kato S., Mutoh I., Shomura M. Collapse of semi-rigidly jointed reticulated domes with initial geometric imperfections. Journal of Constructional Steel Research. 1998, 48 (2-3): 145-168.

Long,H.V, Hung, N.D, (2008): Limit and shakedown analysis of 3-D steel frames, ENGINEERING STRUCTURES, vol. 30, pp.1895-1904.

Maerschalck B.D. and Gerritsma M.I., Higher-Order Gauss–Lobatto Integration for Non-Linear Hyperbolic Equations, Journal of Scientific Computing, Vol. 27, Nos. 1–3, June 2006.

Malla R B., Agarwal P, Ahmad R, Dynamic analysis methodology for progressive failure of truss structures, considering inelastic post-buckling cyclic member behavior. Engineering Structures, 2011,pp 1503-1513.

McGuire W.,Prevention of progressive collapse. Proceedings of the Regional Conference on Tall Buildings. Bangkok:Asion Institute of Technology,(1974)

Melaragno M. An Introduction to Shell Structures: The Art and Science of Vaulting, 1st edition,1991, Van Nostrand Reinhold.

National Institute of Science and Technology (NIST) Final Report on the Collapse of the World Trade Center Towers. NCSTAR 1, Federal Building and Fire 318 Safety Investigation of the World Trade Center Disaster, US Department of Commerce, Gaithersburg, MD, USA(2005).

Office of the Deputy Prime Minister. The building regulations 2000, Part A, Schedule 1: A3, Disproportionate collapse. London (UK); (2004).

Orbison,J.G., Guire M, Abel, J(1982): Yield surface applications in nonlinear steel frame analysis, COMPUTER METHODS IN APPLIED MECHANICS AND ENGINEERING, vol.33, pp.557-573.
Powell G., Progressive collapse: case studies using nonlinear anlysis. SEAOC Annual Convention. Monterey: SEAOC,(2004).

See T., and McConnel R. E., Large Displacement Elastic Buckling of Space Structures, Journal of Structural Engineering, Volume 112 Issue 5 - May 1986.

SEI/ASCE 10-05 Minimum Design Loads for Buildings and Other Structures. Washington, DC: American Society of Civil Engineers, (2010).

SHEKASTEHBAND B., ABEDI K., DYNAMIC PROPAGATION OF SNAP-THROUGH BUCKLING IN TENSEGRITY STRUCTURES, International Journal of Structural Stability and Dynamics Vol. 14, No. 1 (2014) 1350049 (31 pages).

Shimada Y., Matsuoka Y., Yamada S., Suita K. Dynamic collapse test on 3-D steel frame model. The 14th World Conference on Earthquake Engineering, Beijing, (2008).

Starossek U, Progressive collapse of structures: Nomenclature and procedures, Structural Engineering International 16 (2), 113-117.

Starossek,U. Progressive collapse of structures, Thomas Telford Ltd,2009.

Taucer F.F., Spacone E, Filippou F.C., A Fibre beam-column element for seismic response analysis of reinforced concrete structures, A report on research conducted under grant RTA-59M48 from the California Department of Transportation and Grant ECE-8657525 from the National Science Foundation,1991.

Tsitos A., Mosqueda G., Filiatrault A., ReinhornA.M., Experimental investigation of progressive collapse of steel frames under multi_hazard extreme loading. The 14th World Conference on Earthquake Engineering, Beijing,(2008).

Unified Facilities Criteria (UFC)-DoD. Design of Buildings to Resist Progressive Collapse, Department of Defense, (2005).

Yang D.B, Zhang Y.G,Wu J.Z. Elasto-plastic buckling analysis of space truss structures with member equivalent imperfections considered using ABAQUS. Proceedings of the third international conference on modelling and simulation(ICMS2010), p.212-215, (2010).

Zhou H.T, Zhang Y.G,Wu J.Z. Numerical simulation method considering the cumulative effect of plastic damage for beam element. Spatial structures. 2010, 16(3): 13~17.

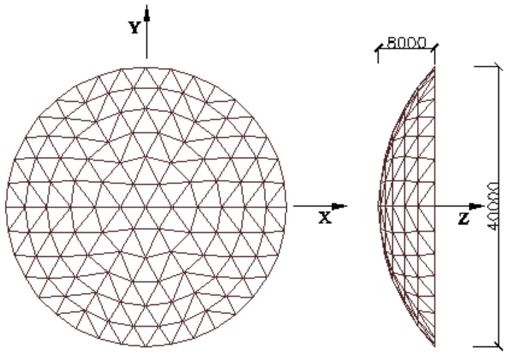

Figure 1 The prototype model

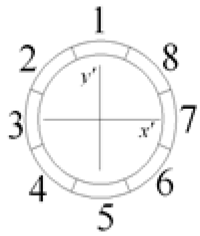

Figure 2 Subdivision of beam element into fibers

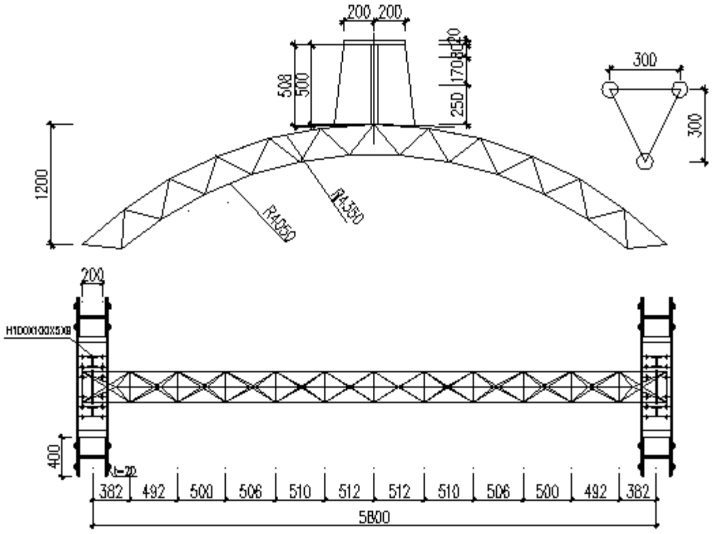

Figure 3 Design drawing of Arch-truss model

Figure 4 Hysteresis loading test on arch-truss

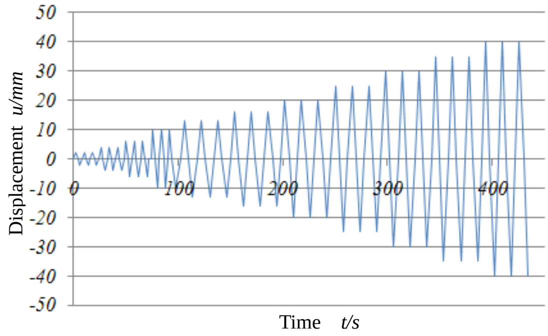

Figure 5 Time history of loading

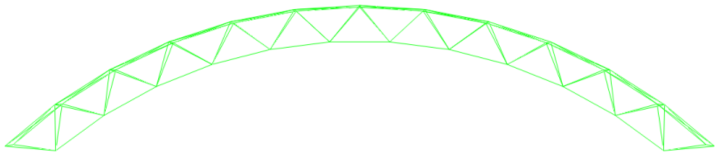

a Main view

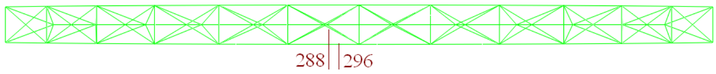

b Top view

Figure 6 Validation Model

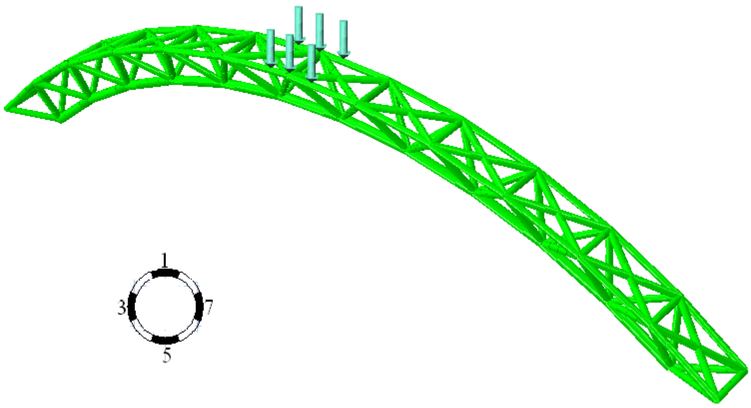

Figure 7 Numerical Model

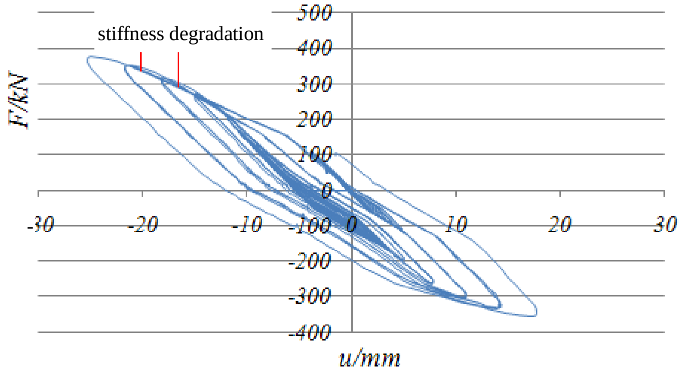

a Hysteric-curve from test

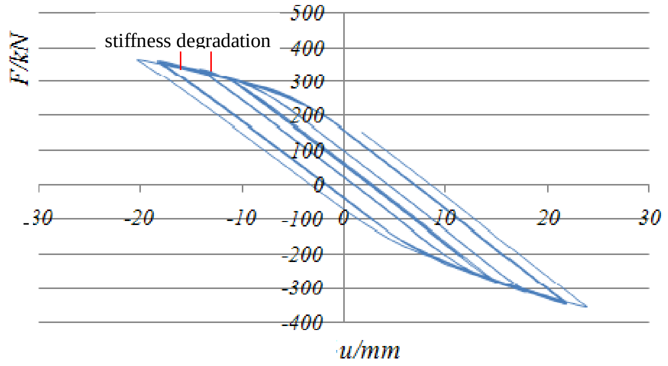

b Hysteric-curve from numerical model

Figure 8 Comparison between the test result and modelling result

a Initial Crack development at support location

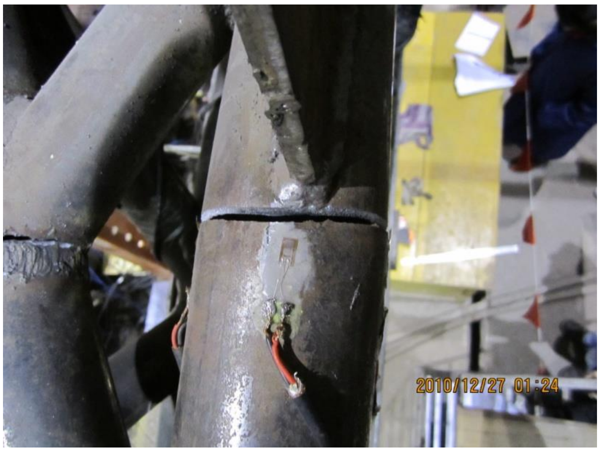

b Further development of the crack at support location

c Crack on the joints of diagonal member

d Fracture at middle of top chord

Figure 9 Fracture process of arch-truss

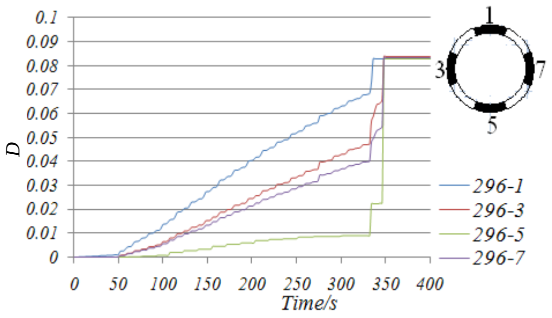

a member 296

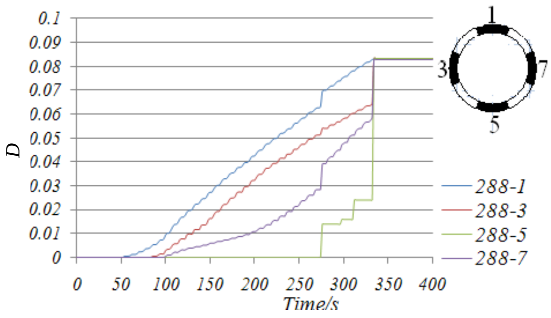

b member 288

Figure 10 Fiber damage - time history curve (showing the result of fiber1, 3, 5, 7 for each element)

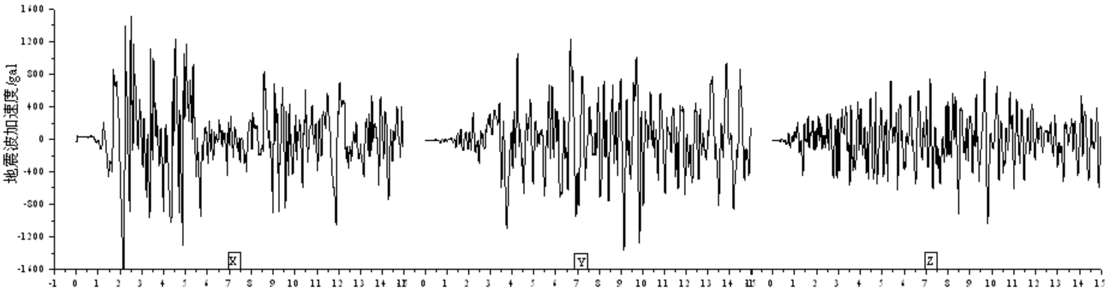

Figure 12 Ground Acceleration-Time history in X, Y and Z direction

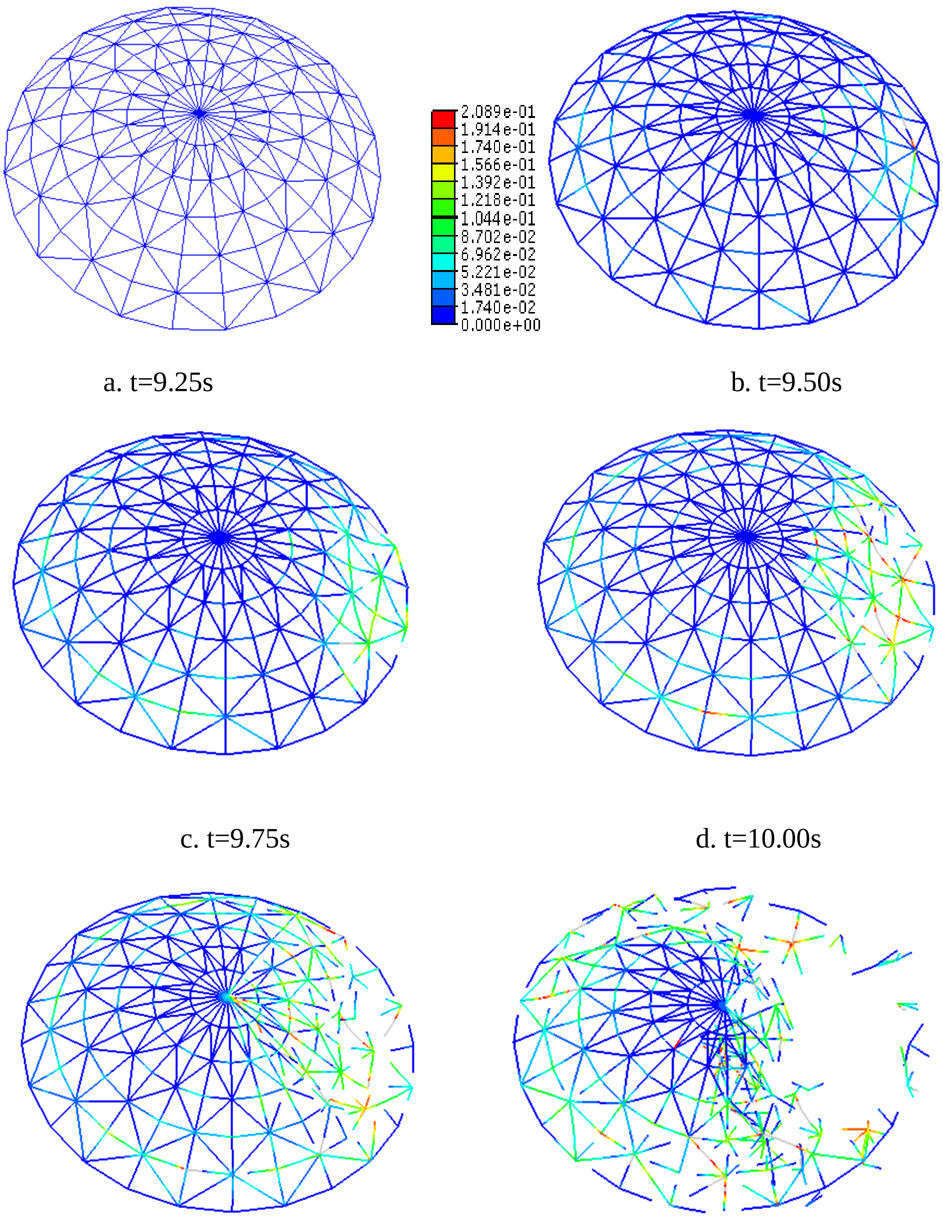

a. t=9.25s

b. t=9.50s

c. t=9.75s

d. t=10.00s

e. t=10.50s

f. t=11.00s

Figure 13 Deformation and damage distribution during collapse process

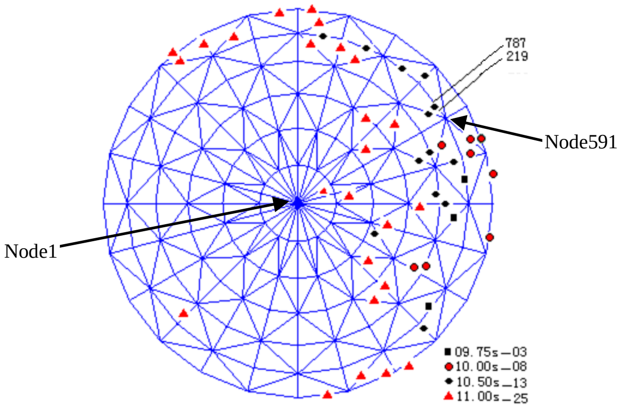

Figure 14 Element failure process

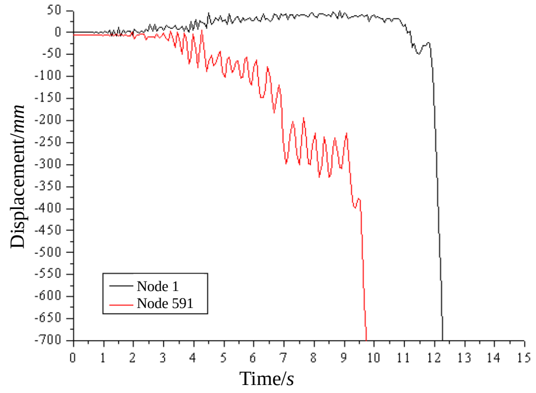

Figure 15 Node displacement-time history curve

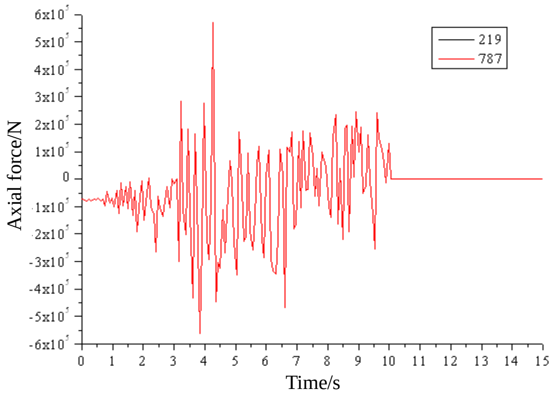

Figure 16 Time history of response of axial force in element 219 and 787

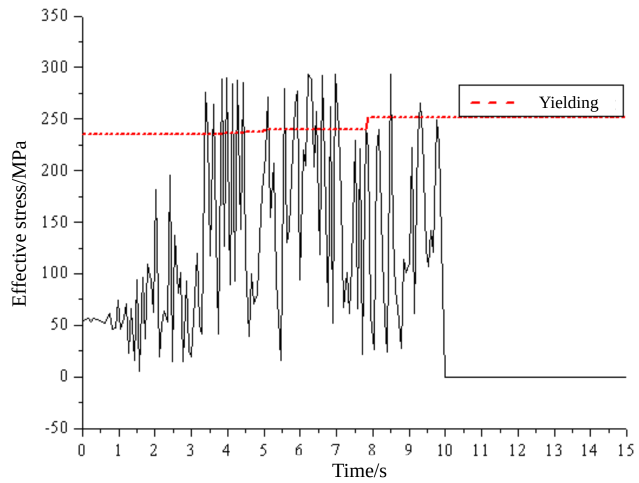

a fiber 0# in element 219

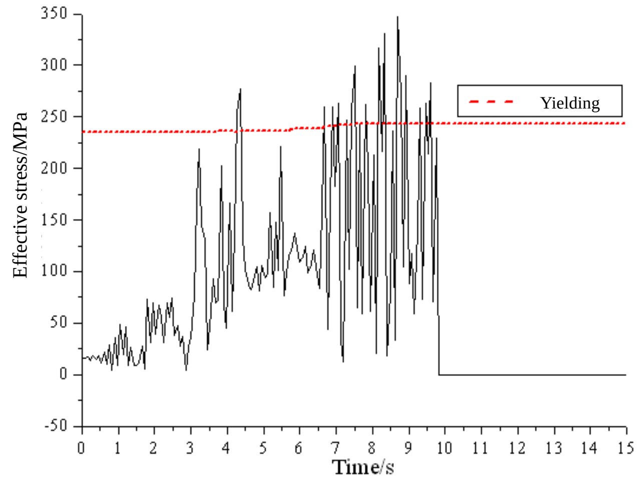

b fiber 90# in element 219

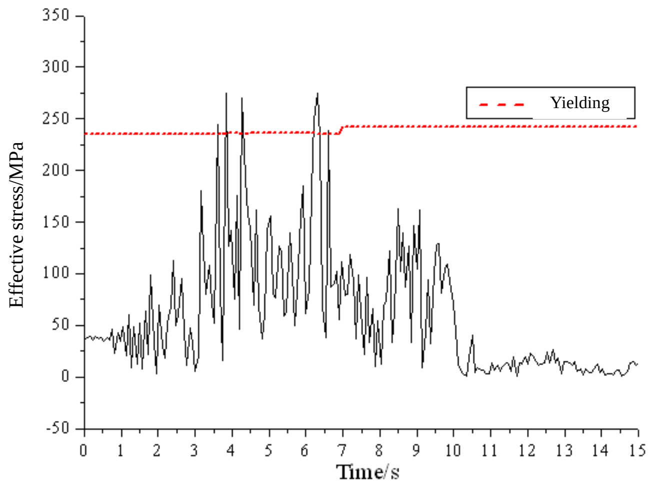

c fiber 0# in element 787

Figure 17 Time history curve of Effective stress in element fiber

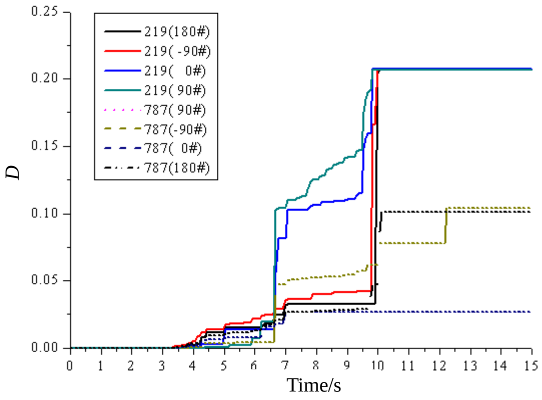

Figure 18 Time history of fiber damage

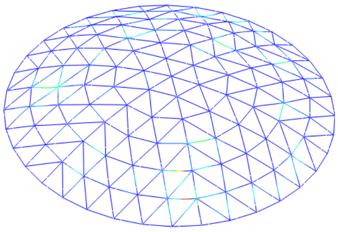

a1 K8 Subsidence appear

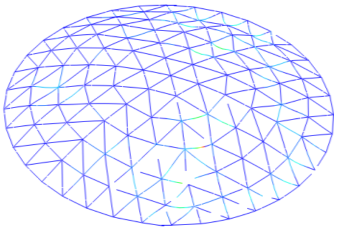

a2 K8 Subsidence develop vertically

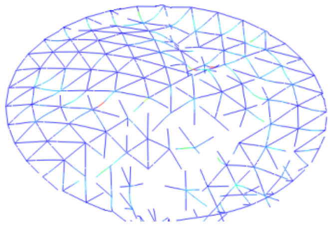

a3 K8 Subsidence develop quickly

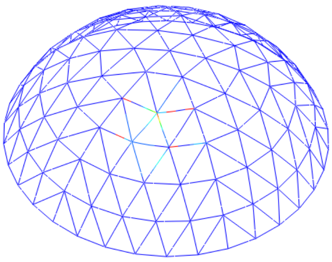

b1 K6 Subsidence appear

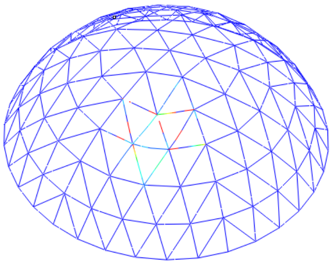

b2 K6 Subsidence develop vertically

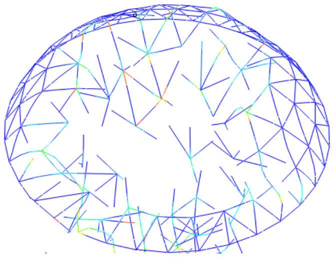

b3 K6 Subsidence develop quickly

Figure 19 Deformation and damage distribution during collapse of Kiewitt shells（a span /depth ratio 7:1，b span/ depth ratio3:1）